Vibrational Spectroscopy of Diimine

Hunter Pauker and Hannah Slocumb

Chem 250L Winter 2021
February 24, 2024

Abstract

The abstract should contain a concise summary of the question/hypothesis investigated (first sentence), state the methods that were used to address it (second sentence), followed by a summary of the most important results (1-2 sentences), and the main conclusions (1-2 sentences). The abstract should be written in present tense.

1 Introduction

The first paragraph of the introduction should explain the broader context of the computational experiment (1-2 sentences) and then funnel the reader towards the research hypothesis/question posed in the lab assignment.

In the second paragraph any relevant existing work in the literature should be referenced, and the relation of this work to the current paper needs to be stated and explained. An original research paper needs to present something new and significant, and explain how its content goes beyond existing work; for a lab report this paragraph can just state key references and sources.

2 Methods

2.1 Statement of the Models

This section introduces theoretical models, equations, assumptions, approximations, etc. that define the theoretical and computational methodology. The section should contain enough information for the paper to be self-contained, no more and no less. Existing methods that have been extensively described elsewhere should not be discussed in detail. For example, it is not recommended to derive the Hartree-Fock equations here.

Symbols or mathematical operators should always be in math mode. Within a text paragraph, use $. For example, the electron charge is e, not e, etc. Simple equations should be typeset using the equation environment, e. g.,

$$i\frac{\partial}{\partial t}\left|\Psi(t)\right\rangle = \hat{H}\left|\Psi(t)\right\rangle. \tag{1}$$

Equations are always a part of complete sentences, with proper punctuation. Separating equations from text by colon or large arrays of equations disconnected from the text should be avoided. All mathematical symbols need to be defined, for example, in Eq. (**??**), $\hat{H}$ could denote the electronic Hamiltonian, and $|\Psi\rangle$ the time-dependent electronic state.

2.2 Computational Details

Here is an example of a computational details section from a recent paper [**Johannson14JPhysChemC118p2**

A global search of the potential energy surfaces of clusters with 9 to 13 gold atoms was performed using a genetic algorithm (GA) [**Hartke.B:ACIE.2002**, **Johnston.R:DT.2003**] based on the formulation by Deaven and Ho [**Deaven.D:PRL.1995**] as implemented in TURBOMOLE [**Sierka.M:ACIE.2007**]. The potential energy surfaces were evaluated at the TPSS (meta-GGA) level [**Tao.J:PRL.2003**] with polarized double-zeta quality def2-SVP basis sets [**Weigend.F:PCCP.2005**, **Weigend.F:PCCP.2006**] and the Stuttgart-Köln 1990 effective core potential (ECP) with 19 valence electrons [**Andrae.D:TCA.1990**]. The resolution of the identity approximation for the Coulomb energy (RI-J method) was used throughout [**Eichkorn.K:CPL.1995**]. The GA optimizations were assumed to be converged if no new minimum structures occurred among the lowest-energy isomers during a certain number of generations. Another indicator of convergence was the presence of both enantiomers for chiral structures. For each cluster size, on the order of 1000 geometry optimizations were necessary to converge the GA search. However, even for extensive GA searches, there is no guarantee that the global minimum is found in a finite number of steps. For completeness, simulated annealing *ab-initio* molecular dynamics simulations [**Elliott00a**] were also performed, but did not generate lower energy structures and failed to find several of the low-energy structures obtained from the GA search.

The thus obtained low-energy structures were subsequently re-optimized at the TPSS level using the triple-zeta quality 7s5p3d1f basis set specifically devised for gold clusters [**Gilb.S:JCP.2002**]. For Au_{11}, this shortened bond lengths by 2-3 pm but did not qualitatively alter the relative isomer energies. All optimized structures were confirmed to be minima by analytical second derivative calculations [**Deglmann04a**, **vanWullen.C:JCC.2011**]. Zero-point vibrational energies and thermal corrections were evaluated using the rigid rotor–harmonic oscillator approximation, after adjusting any very low-energy vibrations (< 10 cm^{-1}) to 10 cm^{-1}.

Final relative energies were obtained from single-point calculations at the converged TPSS/7s5p3d1f structures using all-electron quadruple-zeta quality QZ4P Slater-type basis sets [**vanLenthe.E:JCC.2003**], augmented by two diffuse functions, obtained by dividing the smallest existing s and p exponents by 3.5; these basis sets will be denoted QZ4P(+sp). In the all-electron calculations, relativistic effects were included using the zeroth-order regular approximation (ZORA) [**Chang.C:PS.1986**, **vanLenthe:JCP.1993**] and non-collinear

spin-orbit (SO) corrections [**Eschrig.H:JCC.1999**]. Single-point all-electron ZORA calculations were also performed with the revTPSS meta-GGA functional [**Perdew.J:PRL.2009**]. revTPSS restores the second-order gradient expansion for exchange and produces accurate jellium surface energies. It thus resembles PBEsol [**Perdew.J:PRL.2008**], which significantly outperforms the original PBE GGA [**Perdew.J:PRL.1996**] and rivals the good performance of TPSS for the 2D-3D transition in gold cluster anions [**Johansson.M:PRA.2008**, **Johansson.M:JPCC.2008**]. For the Au_{12}^- anion, single point energies were also computed with the M06-L functional [**M06-L**].

For a lab report, this section can be shorter, but it needs to enable an informed reader to reproduce the results. As opposed to other sections, which are best written in present tense, the computational details section should be in simple past.

3   Results

This section should report all results relevant to the hypothesis/question introduced above. Rather than supplying "commented Gaussian output" or all raw data, the section must be structured and discuss the data in an intelligible way. Smaller data sets (up to ~ 20 entries) are best reported as tables, larger and multivariate data sets are best reported as figures.

Tab. **??** is a slightly modified example from Ref. [**Johannson14JPhysChemC118p29370**]. Rules and other lines should be used sparingly. Columns containing numerical data should be in math mode to ensure, e.g., that minus signs are displayed as $-$, not - (dash). The caption defines the data shown in all columns, including their units, and is relatively self-contained. Thus, a reader with much background knowledge can retrieve important information quickly by just reading the abstract and the tables, figures, and their captions. Separate table or figure notes are best avoided if possible, but if you need to use them, they may be generated by enclosing the float into a minipage environment and using the footnote command.

	2D?		PBEsol	TPSS	RPA	revTPSS	$\Delta G(100K)$
Au_8^+-I		C_{2v}	0	0	0	0	0
II		C_s	$+7.1$	$+2.4$	$+0.7$	$+10.2$	$+8.1$
III	$\surd$	D_{2h}	$+16.7$	$+8.7$	$+17.4$	$+26.4$	$+24.6$
IV	$\surd$	C_{2v}	$+17.8$	$+12.7$	$+11.3$	$+27.1$	$+23.8$
Au_{12}^--I		C_{2v}	0	0	0	0	0
II	$\surd$	D_{3h}	-9.1	-19.5	-6.8	$+1.9$	$+1.0$

Table 1: Dimensionalities, point groups, relative energies at 0 K (kJ/mol) between the energetically lowest 2D and 3D structures for Au_8^+ and Au_{12}^-; all relative energies include the vibrational zero-point-energy and spin-orbit coupling, the computed free energy differences $\Delta G(100K)$ are based on revTPSS electronic energies.

When making figures, vector graphics (svg, eps, and native pdf formats) is always prefer-

able for simple plots and diagrams, because it allows scaling without quality loss. For images, complex molecular visualizations such as orbital plots or rendered molecular graphics, bitmaps such as png or jpg are used.

Fig. **??** shows an example from [**Vincent16JPhysChemLett7p4185**] containing vector graphics figures. The optional width argument of the includegraphics command allows
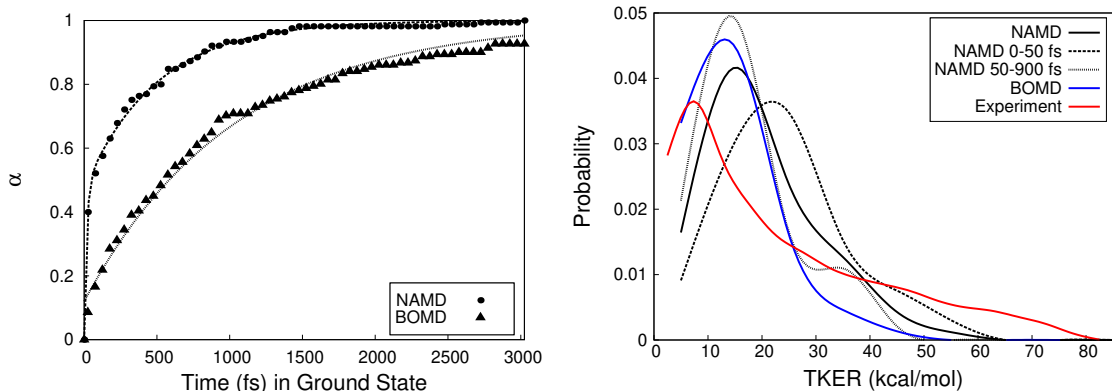

Figure 1: (a) Degree of C–H dissociation α for channels (1)–(3) as a function of time spent in the S_0 state. Grey dotted curves indicate mono- (BOMD) and biexponential (NAMD) fits. (b) Comparison of the experimental TKER probability distributions [**Lee09JChemPhys131p174312**] (purple) for the H-loss channels (1)-(3) to BOMD (blue) and NAMD (gray) simulations. The NAMD TKER distribution is the sum of TKER resulting from fast (0-50 fs) and slow (50-3000 fs) dissociations.

specification of the figure width while keeping the aspect ratio.

It is not recommended to "pin" floats such as tables and figures to certain places in the text. Rather, the optional arguments of the table or figure environment should be used to specify the preferred alignment (in order of priority), e.g., h for "here", t for "top", b for bottom of a page, and p for a separate page containing floats only.

The text may guide the reader through the results and discuss them, but should not merely re-state the contents of the tables and figures.

4 Conclusions

This section should aim to answer the hypothesis or question stated in the introduction clearly and concisely, as well as other possibly significant results of the study. Do not provide a summary of your work here, the correct place for that is the abstract. Instead, the conclusions must explain what has been learned, and how it is relevant to the initial question.

Acknowledgments

This section should acknowledge any additional sources of support from professionals who aren't co-authors but helped you complete your work. For example, O. H. would like to acknowledge useful discussions with The Three Stooges. Often, funding agencies mandate that funding be acknowledged in this section.